Micro-Doses of DNP Preserve Motor and Muscle Function with a Period of Functional Recovery in Amyotrophic Lateral Sclerosis Mice

Renjia Zhong, MD, PhD,[1,2,3] Demi L.A. Dionela, BS,[1] Nina Haeyeon Kim, MS,[1] Erin N. Harris, BS,[1] John G. Geisler, PhD,[4] and Lan Wei-LaPierre, PhD[1,2,5]

Objective: Mitochondrial dysfunction is one of the earliest pathological events observed in amyotrophic lateral sclerosis (ALS). The aim of this study is to evaluate the therapeutic efficacy of 2,4-dinitrophenol (DNP), a mild mitochondrial uncoupler, in an ALS mouse model to provide preclinical proof-of-concept evidence of using DNP as a potential therapeutic drug for ALS.
Methods: hSOD1^{G93A} mice were treated with 0.5–1.0 mg/kg DNP through daily oral gavage from presymptomatic stage or disease onset until 18 weeks old. Longitudinal behavioral studies were performed weekly or biweekly from 6 to 18 weeks old. In situ muscle contraction measurements in *extensor digitorum longus* muscles were conducted to evaluate the preservation of contractile force and motor unit numbers in hSOD1^{G93A} mice following DNP treatment. Muscle innervation and inflammatory markers were assessed using immunostaining. Extent of protein oxidation and activation of Akt pathway were also examined.
Results: DNP delayed disease onset; improved motor coordination and muscle performance in vivo; preserved muscle contractile function, neuromuscular junction morphology, and muscle innervation; and reduced inflammation and protein oxidation at 18 weeks old in hSOD1^{G93A} mice. Strikingly, symptomatic hSOD1^{G93A} mice exhibited a period of recovery in running ability at 20 cm/s several weeks after 2,4-dinitrophenol treatment started at disease onset, offering the first observation in disease phenotype reversal using a small molecule.
Interpretation: Our results strongly support that micro-dose DNP may be used as a potential novel treatment for ALS patients, with a possibility for recovery, when used at optimal doses and time of intervention.

ANN NEUROL 2024;00:1–16

Amyotrophic lateral sclerosis (ALS) is a devastating neurodegenerative disease characterized by progressive motor neuron (MN) loss, muscle denervation and eventually paralysis. The majority of ALS cases are sporadic (sALS), with 10% of cases being familial (fALS). There are several different genetic causes of fALS, including mutations in Cu, Zn, superoxide dismutase (SOD1), Chromosome 9 open reading frame 72, RNA binding protein Fused in Sarcoma and TAR DNA binding protein (TARDBP).[1–4] There are currently no effective treatments to stop or reverse ALS disease progression. The 3 FDA approved drugs to treat ALS (Riluzole,[5] Edaravone,[6] and

View this article online at wileyonlinelibrary.com. DOI: 10.1002/ana.27140

Received Jun 14, 2024, and in revised form Oct 28, 2024. Accepted for publication Nov 2, 2024.

Address correspondence to Dr Wei-LaPierre, Department of Applied Physiology and Kinesiology, College of Health and Human Performance, University of Florida, 1864 Stadium Road, Gainesville, FL, 32611. E-mail: lweilapierre@ufl.edu

From the [1]Department of Applied Physiology and Kinesiology, College of Health and Human Performance, University of Florida, Gainesville, FL; [2]Department of Pharmacology and Physiology, School of Medicine and Dentistry, University of Rochester, Rochester, NY; [3]Department of Emergency Medicine, the First Affiliated Hospital of China Medical University, Shenyang, China; [4]Mitochon Pharmaceuticals Inc, Blue Bell, PA; and [5]Myology Institute, University of Florida, Gainesville, FL

Additional supporting information can be found in the online version of this article.

AMX0035[7]) either extend survival by 3–6.5 months or only show efficacy in a small subset of early stage ALS patients. The newly United States Food and Drug Administration (FDA) -approved hSOD1^{G93A} antisense oligonucleotide (Tofersen) for ALS patient carrying the hSOD1 mutation did not show improvement in ALS Functional Rating Scale (ALSFRS-R) in Phase III trial, while reduced the expression of a neurodegeneration biomarker, neurofilament light.[8] Therefore, identification of an effective treatment for ALS is imperative. Although the molecular mechanism underlying ALS remains unclear, mitochondrial dysfunction is identified as an early pathology. Decreased mitochondrial respiratory chain activity, altered mitochondrial ultrastructure, and mitochondrial dysfunction in MNs and skeletal muscle are widely reported in patients with ALS[9–11] and in the brain, spinal cord, MN terminals, and skeletal muscle of most ALS transgenic mouse models.[12–14] The mechanisms leading to global mitochondrial dysfunction remain unclear. One possibility is mitochondrial Ca^{2+} dysregulation, leading to the opening of mitochondrial membrane permeability transition pore (mPTP) and cell death. Abnormal mitochondrial Ca^{2+} accumulation is implicated in the pathogenesis of neurodegenerative conditions such as spinobulbar muscular atrophy, Alzheimer's disease, Parkinson's disease, and ALS.[15,16]

2,4 dinitrophenol (DNP) is a weak mitochondrial uncoupler that was previously used to increase energy expenditure to promote weight loss in humans in the 1930s at high doses (~300 mg/day). At low doses, DNP slightly dissipates mitochondrial membrane potential ($\Delta\Psi_m$) and reduces the driving force for mitochondrial Ca^{2+} uptake, which indirectly reduce the amplitude of mitochondrial Ca^{2+} influx. Over the past decade, accumulating evidence indicates that low-dose (0.5-5 mg/kg), weight-neutral DNP is pan-neuroprotective[17–19] and improves treatment outcomes for traumatic brain injury[20] possibly due to its inhibition of mitochondrial Ca^{2+} influx and reactive oxygen species (ROS) production, while promoting repair with induction of brain derived neurotrophic factor (BDNF).[21] DNP (or MP101, manufactured by Mitochon Pharmaceuticals under the guideline of Good Manufacture Practice) was recently granted an "investigative new drug" status by the FDA due to its neuroprotective potential and Good Laboratory Practice toxicology profile at low doses.

In this study, we examined the therapeutic efficacy of DNP on preventing MN loss and preserving muscle innervation and contractile function in hSOD1^{G93A} ALS mice. Micro-dose DNP (0.5–1 mg/kg, human equivalent dose of 2.5–5 mg/day, similar dose to previously studies, determined by pharmacokinetic analysis[22,23]) treatment in ALS hSOD1^{G93A} mice elicited global protective effects in motor function, with potential recovery in phenotype after disease onset, providing critical proof-of-concept evidence on the protective effect of DNP in modifying the ALS disease phenotype.

Materials and Methods

Animals

All procedures conducted in the study are in accordance with the guidelines of Institutional Animal Care and Use Committee and approved by the University of Rochester and University of Florida. Wild-type (WT) and hSOD1^{G93A} mice on congenic C57BL/6J background were used for this study. HSOD1^{G93A} mice breeders were obtained from The Jackson Laboratory, and a colony was established and maintained in a pathogen-free facility with a light/dark cycle of 12 h at constant temperature and humidity at the University of Rochester and University of Florida. Food and water were provided ad libitum. Experimental groups were randomized, and researchers were blinded to mouse identity and treatments. Both male and female mice were included in each experimental group. A priori power calculations ($\alpha = 0.05$; power = 0.8) of sample size based on standard deviation of the preliminary data were used to determine the number of animals required for each experiment. Age/sex matched WT littermates were used as controls.

DNP (MP101) Treatment

Doses of 0.5 and 1.0 mg/kg DNP and vehicle control were administered daily through oral gavage, starting from 4 weeks (early presymptomatic) or 10 weeks of age (disease onset) until experimental endpoint at 18 weeks old (Fig 1A, blue dots). Separate cohorts of hSOD1^{G93A} mice and WT littermates were used for each dose, each time point.

Behavioral Analysis

A battery of longitudinal behavioral studies, including accelerating rotarod tests, fixed speed rotarod tests, running ability, wire hang tests, and hang & escape tasks were performed on hSOD1^{G93A} mice and WT controls from the age of 6 weeks old until 18 weeks old, as described previously.[24,25] Vehicle- (Veh-) and DNP-treated mice from each experimental group starting DNP treatment from 4 weeks old were assessed for disease onset using accelerating rotarod (accelerating 4–40 rpm in 300 seconds) once a week from 6 to 10 weeks. Fixed speed rotarod (5–37 rpm, more suitable to resolve subtle functional defect compared with accelerating rotarod), wire hang, and hang escape test were performed at 14, 16, and 18 weeks of age to track disease progression after disease onset (Fig 1A, Pink dots). Mouse running ability at 20 cm/s was assessed using a DigiGait apparatus. Mice were allowed to run on the treadmill of the apparatus and a video was recorded from underneath the treadmill belt. Successful completion of a run at 20 cm/s was defined as having a compliant video (running at consistent gait for 3–5 seconds) recorded.

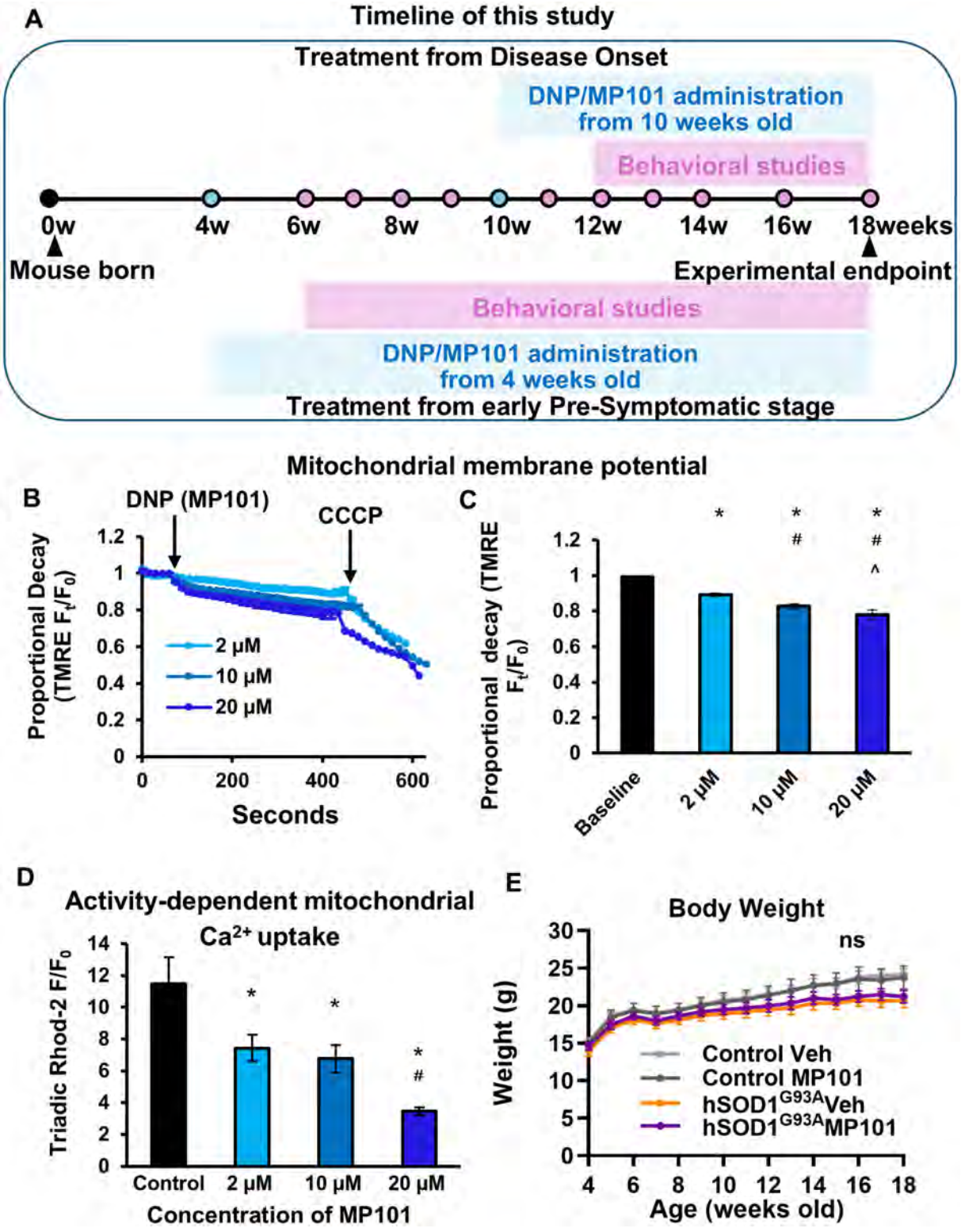

FIGURE 1: Experimental timeline and dose-dependent reduction of mitochondrial membrane potential and mitochondrial Ca^{2+} uptake by DNP. (A) DNP/MP101 administration and experimental timeline. (B) Averaged time-lapsed traces for mitochondrial membrane potential ($\Delta\Psi_m$) measurements during the application of 2–20 μM of DNP (MP101) and 1 μM CCCP. (C-D) Averaged (±SEM) dose-dependent decrease in $\Delta\Psi_m$ at the end of DNP (MP101) application (C) and peak amplitude of mitochondrial Ca^{2+} uptake in response to 5 tetanic electrical stimulations at 100 Hz in the presence of 2–20 μM DNP/MP101 (D). (E) Averaged (±SEM) body weight of WT and hSOD1^{G93A} mice treated with 0.5–1 mg/kg MP101 or Veh up to 18 weeks old. *$p < 0.05$ versus baseline/control; #$p < 0.05$ versus 2 μM MP101; ^$p < 0.05$ versus 10 μM MP101; 1-way ANOVA with Tukey post hoc test. n = 6–8 cells from 2 to 3 mice (B-D); 1-way ANOVA with Tukey post hoc test. N = 5–8 mice (E).

In Situ Muscle Contractile Force Measurements

In situ muscle contraction approach was employed to assess isometric frequency-dependent force generation in *extensor digitorum longus* (EDL, fast twitch, ALS susceptible) muscles for neuromuscular junction (NMJ) transmission and muscle contractile function. Anesthetized Veh- and DNP-treated WT and hSOD1^{G93A} mice were placed on a custom-made stage heated to 37°C, with hind limb stabilized. The distal tendon of EDL muscle was attached to a 409C force transducer (Aurora scientific). A force-frequency curve was generated by stimulating the peroneal nerve at 1 (single twitch), 25, 50, 75, 100, 125, 150, and 175 Hz for 500 ms contractions with 1 minute rest in between contractions.

Motor Unit Number Estimation (MUNE)

Motor unit (MU) number was determined using in situ muscle contraction as previously described.[26] A series of twitch contractions were measured while stimulating the peroneal nerve while progressively increasing stimulus strength (single 0.1 ms pulses delivered every 30 seconds with stimulation currents increased at 5 μA increments). As the stimulation current increases, more motor units were recruited into the contraction, shown as stepwise increases in twitch contractile force. The use of very small current increments (5 μA) enables resolution of the recruitment of individual MU. Recruitment was complete when twitch force was maximal. The number of discrete steps of increase in contractile force were counted and reported as MUNE.

NMJ Structure/Denervation Analysis

To assess muscle innervation, EDL muscles from Veh- or DNP-treated WT and hSOD1^{G93A} mice were stained for presynaptic/postsynaptic markers, as previously described.[27] EDLs were fixed, permeabilized, blocked, and probed in a primary antibody cocktail against neurofilament and presynaptic proteins (see Supplemental Table 1 for antibody details) for 24 hours at 4°C, followed by Alexa 568 anti-mouse secondary antibodies and Alexa 488-conjugated bungarotoxin to visualize presynaptic and postsynaptic (acetylcholine receptor [AChR]) structures, respectively.

Images of NMJ staining were acquired using a Leica Stellaris 5 confocal microscope. Stacks of x-y images were acquired with a step size of 0.5 μm for NMJs throughout the entire EDL muscle. A minimum of 200 NMJs were evaluated for each muscle to ensure a thorough examination of innervation. Researchers conducting the analysis were blinded of sample phenotypes and treatments. Areas rich in AChR staining were analyzed for postsynaptic fragmentation (with ≥4 AChR islands in 1 NMJ),[28] degeneration, complexity ("pretzel" or "plaque" shaped) and pre/post-synaptic staining overlap (innervation). The criteria for defining innervation/denervation are: fully innervated, presynaptic/postsynaptic apparatus overlap 100%; partially innervated: >50% overlap; and denervated, <50% overlap.

Measurements of $\Delta\Psi_m$ in Flexor Digitorum Brevis (FDB) Muscle Fibers

FDB fibers were isolated using enzymatic digestion in Collagenase A and $\Delta\Psi_m$ measured as previously described.[29] Tetramethylrhodamine ethyl ester (TMRE)-loaded FDB fibers were locally perfused with 2, 10, and 20 μM of DNP for 7 minutes before $\Delta\Psi_m$ was fully collapsed by application of 1 μM carbonyl cyanide 3-chlorophenylhydrazone (CCCP) as a positive control.

Activity-Dependent Mitochondrial Ca^{2+} Uptake in FDB Fibers

Rhod-2-loaded FDB fibers were incubated with corresponding concentration of DNP for 10 minutes and then electrically stimulated at 100 Hz for 5 times to elicit mitochondrial Ca^{2+} uptake, measured as previously described.[29]

Immunofluorescence Staining

Macrophage infiltration was examined using CD68 in EDL cryosections.[30] Sections were probed with anti-CD68 and anti-laminin antibodies overnight at 4°C. DAPI (4',6-diamidino-2-phenylindole) was included in the secondary antibody solution to visualize nuclei. Immunofluorescent images were obtained using an Invitrogen Evos cell imaging system and analyzed off-line using Image J.

Immunobloting

Western blot and immunostaining were conducted as previous[31] in tibialis anterior (TA) muscles from hSOD1^{G93A} and WT mice treated with 0.5 mg/kg DNP from disease onset for expression of total Akt and phosphorylated Akt (pAkt, Ser473) (see Supplemental Table 1 for antibody details). Oxyblot was performed using Protein Carbonyl Assay Kit (Abcam) as per manufacture instructions. Glyceraldehyde-3-phosphate-dehydrogenase (GAPDH) and ponceau total protein stain were used as loading controls for Akt and Oxyblot, respectively.

Statistical Analysis

Results were expressed as mean ± SEM and statistical analysis conducted using Graphpad Prism 10.2 software. One-way analysis of variance (ANOVA) or 2-way ANOVA with repeated measures followed by Tukey post hoc tests were used as appropriate. The recovery of running ability at 20 cm/s was analyzed using Fischer's exact test. The value of $p < 0.05$ was considered statistically significant.

Results

DNP (MP101) Reduces $\Delta\Psi_m$ and Activity-Dependent Mitochondrial Ca^{2+} Uptake in a Dose Dependent Manner in FDB Fibers

The effect of DNP, or MP101, on $\Delta\Psi_m$ and mitochondrial Ca^{2+} uptake was first validated in acutely isolated FDB muscle fibers. Seven minutes of exposure of TMRE-loaded FDB fibers to 2–20 μM MP101 revealed a

10–20% reduction in $\Delta\Psi_m$ indicated by TMRE fluorescence in a dose-dependent manner (Fig 1B,C). Activity-dependent mitochondrial Ca^{2+} uptake exhibited a marked reduction in the amplitude of mitochondrial Ca^{2+} uptake following 2 μM MP101, with a further decrease observed when exposed to 20 μM MP101 (Fig 1D). These results validate the inhibitory effect of MP101 on mitochondrial Ca^{2+} uptake in skeletal muscle cells.

Treatment with 0.5 mg/kg MP101 Delayed Disease Onset and Progression in hSOD1^{G93A} ALS Mice

WT and hSOD1^{G93A} mice were treated with 0.5 mg/kg MP101 or Veh started from either early presymptomatic stage (4 weeks old) or at disease onset (10 weeks old). No MP101-associated weight loss was observed up to experimental endpoint at 18 weeks old (Fig 1E), validating that the dosages used in this study are weight-neutral. Veh-treated hSOD1^{G93A} mice showed a decline in motor coordination from as early as 7 weeks old, measured by accelerating rotarod, while this decline was delayed to after 9 weeks old in mice treated with 0.5 mg/kg MP101 started from 4 weeks old (hSOD1^{G93A} MP101, Fig 2A). After disease onset, MP101-treated hSOD1^{G93A} mice exhibited improved motor coordination assessed by fixed speed rotarod test at 14, 16, and 18 weeks old at high speed at 37 rpm (Fig 2B). Treatment with MP101 at 1.0 mg/kg from 4 weeks old offered similar protective effect in motor coordination in hSOD1^{G93A} mice up to 18 weeks old (Fig 2C).

Next, we examined the effect of MP101 with treatment starting from disease onset (10 weeks old). This time point is highly clinically relevant due to the fact that majority of patients with ALS first approach their physicians after experiencing symptoms. hSOD1^{G93A} mice showed similar baseline phenotypes before the start of treatment at 10 weeks old using rotarod assessment (Fig 3A, shaded area). Treatment with 0.5 mg/kg MP101 from 10 weeks old prevented functional decline in hSOD1^{G93A} mice until 14 weeks old (at speed higher than 31 rpm) and significantly improved motor coordination at all 14, 16m and 18 weeks old at higher than 20 rpm compared with veh-treated age/sex-match littermates (Fig 3A). Application of 1.0 mg/kg MP101 also preserved motor coordination after disease onset until experimental endpoint (Fig 3B). Further, the mice treated with MP101 from 10 weeks old were evaluated for their ability to run at 20 cm/s. hSOD1^{G93A} mice typically lose this ability around 10–12 weeks old due to disease progression. The measurements started from 7 weeks old to record a baseline before the treatments started. The probability of the mice completing the task was significantly higher in the MP101-treated mice compared with Veh-treated group (Fig 3C), with the latter having no mice being able to run at this speed after 13 weeks old. One MP101-treated mouse was able to run at 20 cm/s throughout the entire time course until experimental endpoint. Remarkably, in hSOD1^{G93A} mice treated with 0.5 mg/kg MP101, ~70% of mice regained the running ability for 1–2 weeks (equivalent to human life ~300–600 days) after MP101 started (Fig 3C, green checked bars indicate the percentage of recovered mice for each week), while none of the Veh-treated hSOD1^{G93A} mice regained this ability (Fig 3D, categorical data showing the overall recovery rate, $p = 0.012$ Fischer's exact test; for detailed recovery data, please see supplemental Fig 1). This result provides compelling evidence on the rescuing effect of MP101 on motor function in symptomatic hSOD1^{G93A} mice.

MP101 Treatment from Both Presymptomatic Stage and Disease Onset Improved Overall Muscle Strength in hSOD1^{G93A} ALS Mice

Treatment with 0.5 mg/kg MP101 improved sustained grip strength (wire hang tests) at 16 and 18 weeks old when treatment started from both presymptomatic (Fig 4A) or disease onset (Fig 4B). Similar protection in muscle strength was observed in mice treated with 1.0 mg/kg from disease onset (Fig 3C). Hang escape task is an assessment of whole-body strength. Treatment with MP101 prevented the decline in performance in this test in hSOD1^{G93A} mice at 18 weeks old. This functional improvement was observed in mice treated with MP101 from both 4 weeks and 10 weeks old, at dosages of both 0.5 mg/kg and 1.0 mg/kg (Fig 4D-F). A comparison between treatment paradigms at 18 weeks old revealed comparable protection across all treatments with both wire hang and hang escape task, regardless of time to start treatments or the dosages (Fig 4G,H).

MP101 Treatment Improved Muscle Contractile Function at 18 Weeks Old in hSOD1^{G93A} ALS Mice

In situ muscle peak contractile force was measured in EDL muscles at 18 weeks old in Veh- and MP101-treated hSOD1^{G93A} and WT mice to evaluate the protective effect of MP101 on muscle strength in individual muscles. Force frequency analysis showed a global rescue of force production in all higher frequencies in all treatments that we applied, starting from both 4 weeks and 10 weeks old at both dosages (Fig 5, % rescue ~31%, 38%, 33%, and 35% in B-E, respectively).

MP101 Treatment Preserved Motor Unit Number at 18 Weeks Old in hSOD1^{G93A} ALS Mice

A decrease in the number of motor units (MUs) that occurs prior to detectable changes in muscle strength is an early

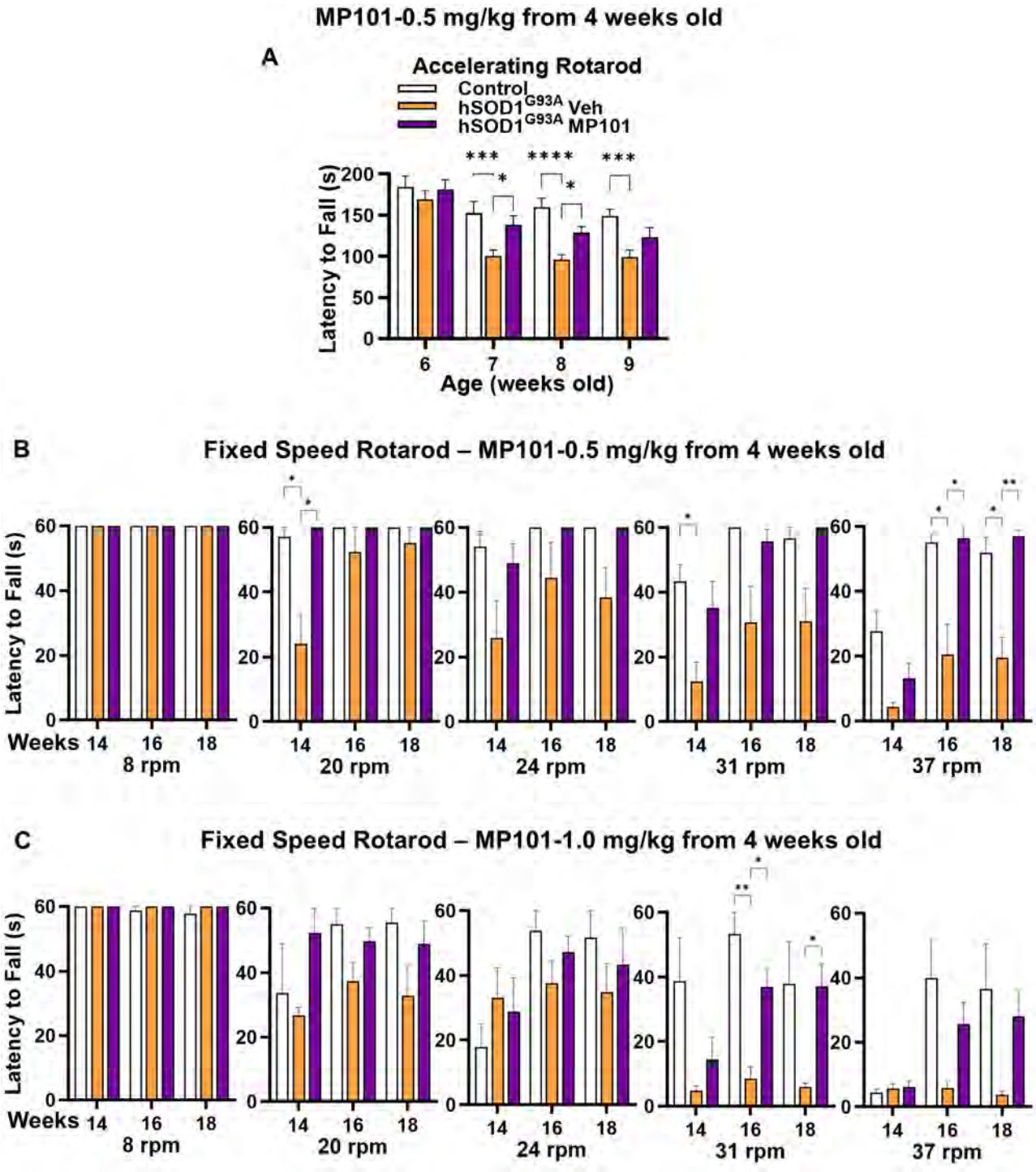

FIGURE 2: Treatment with MP101 from early presymptomatic stage delayed disease onset and progression in hSOD1^{G93A} ALS mice. (A) Averaged (±SEM) latency to fall during motor coordination test using accelerating Rotarod (4–40 rpm in 300 seconds) in 0.5 mg/kg MP101 and Veh-treated hSOD1^{G93A} and age/sex matched WT mice from 4 weeks old to determine disease onset. (B) Averaged (±SEM) latency to fall during fixed-speed Rotarod motor coordination test at 14, 16, and 18 weeks old in the same cohorts of mice in A to assess disease progression. (C) Averaged (±SEM) latency to fall during fixed-speed Rotarod motor coordination test at 14, 16, and 18 weeks old in WT and hSOD1^{G93A} mice treated with Veh or 1.0 mg/kg MP101 from 4 weeks old presymptomatic stage. *$p < 0.05$, **$p < 0.01$, ***$p < 0.001$, 2-way ANOVA with repeated measures, Tukey post hoc test. N = 8–13 mice (3–5 males and 5–8 females) for A and B; N = 7–10 mice (2–4 males and 5–6 females) for C. No difference was observed between WT mice treated with Veh and MP101. Therefore, these groups were combined as "Control" group. This combined control group applies for the rest of the study.

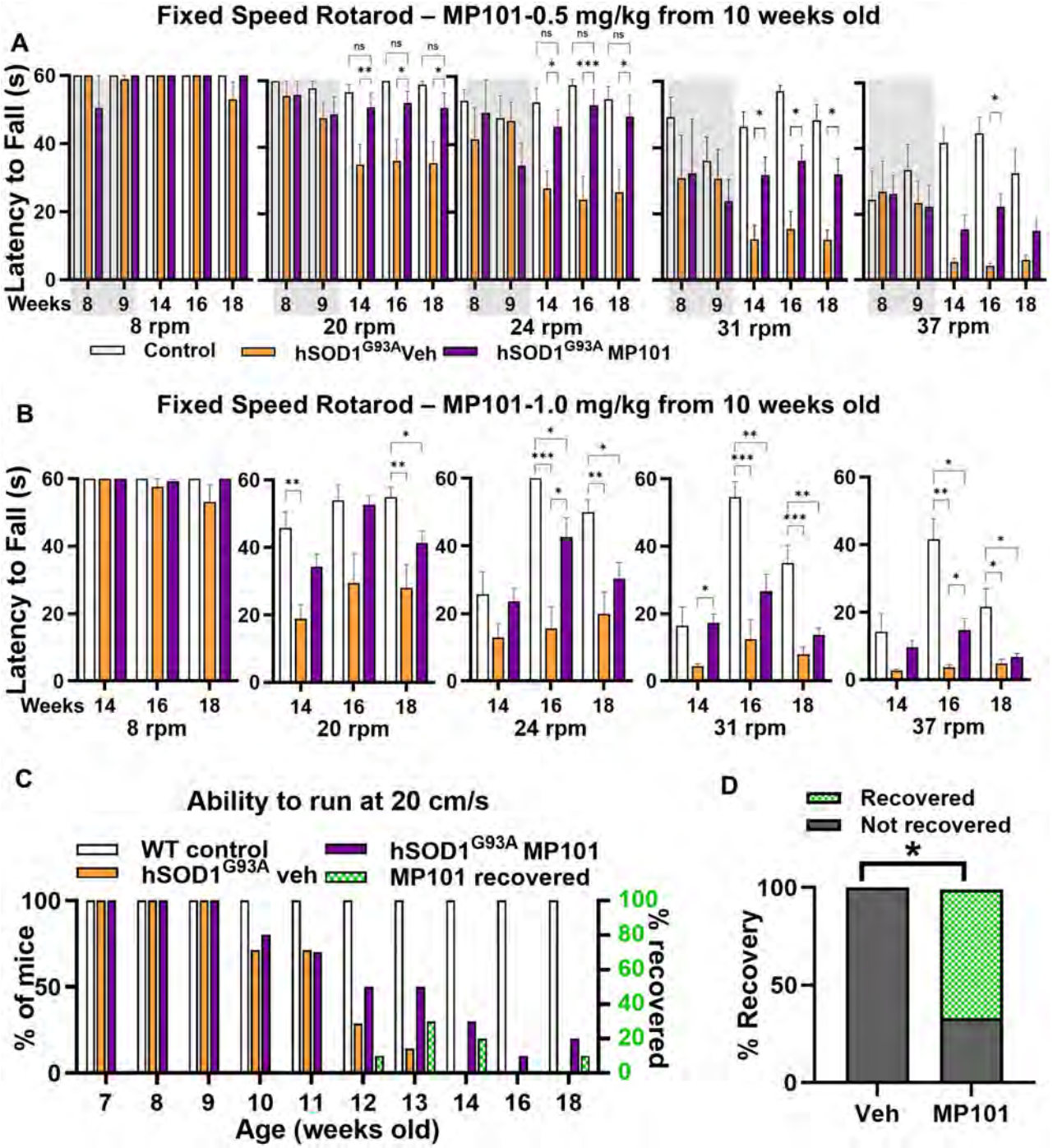

FIGURE 3: Treatment with MP101 from 10 weeks old at disease onset delayed disease progression and promoted recovery of running ability in hSOD1^{G93A} ALS mice at advanced stage. (A) Averaged (±SEM) latency to fall during longitudinal fixed-speed Rotarod coordination tests at speed 8–37 rpm in age/sex matched 0.5 mg/kg MP101 and Veh-treated hSOD^{G93A} and WT mice. Shaded areas indicate measurements recorded before the start of MP101 treatment to ensure the same pretreatment baseline in the hSOD1^{G93A} mice in disease stages. (B) Averaged (±SEM) latency to fall during fixed-speed Rotarod motor coordination test at 14, 16, and 18 weeks old in WT and hSOD1^{G93A} mice treated with Veh or 1.0 mg/kg MP101 from 10 weeks old. (C) Averaged percentage of mice completed 20 cm/s running test (using DigiGait apparatus) at the given time points in hSOD1^{G93A} mice treated with Veh or 0.5 mg/kg MP101 from 10 weeks old. Green checkered bars (on right Y axis) indicate percentage of mice recovered for the corresponding time point after previously lost the ability of running at 20 cm/s. (D) Total percentage of mice recovered (checkered bars) and never recovered (*solid gray*) in hSOD1^{G93A} mice treated with 0.5 mg/kg MP101 or Veh at 10–18 weeks old. (A-B), *$p < 0.05$, **$p < 0.01$, ***$p < 0.001$, 2-way ANOVA with repeated measures, Tukey post hoc test. N = 10–12 mice; (C-D), Fischer exact test. *$p < 0.05$, N = 7–10 mice (3–4 males and 4–6 females).

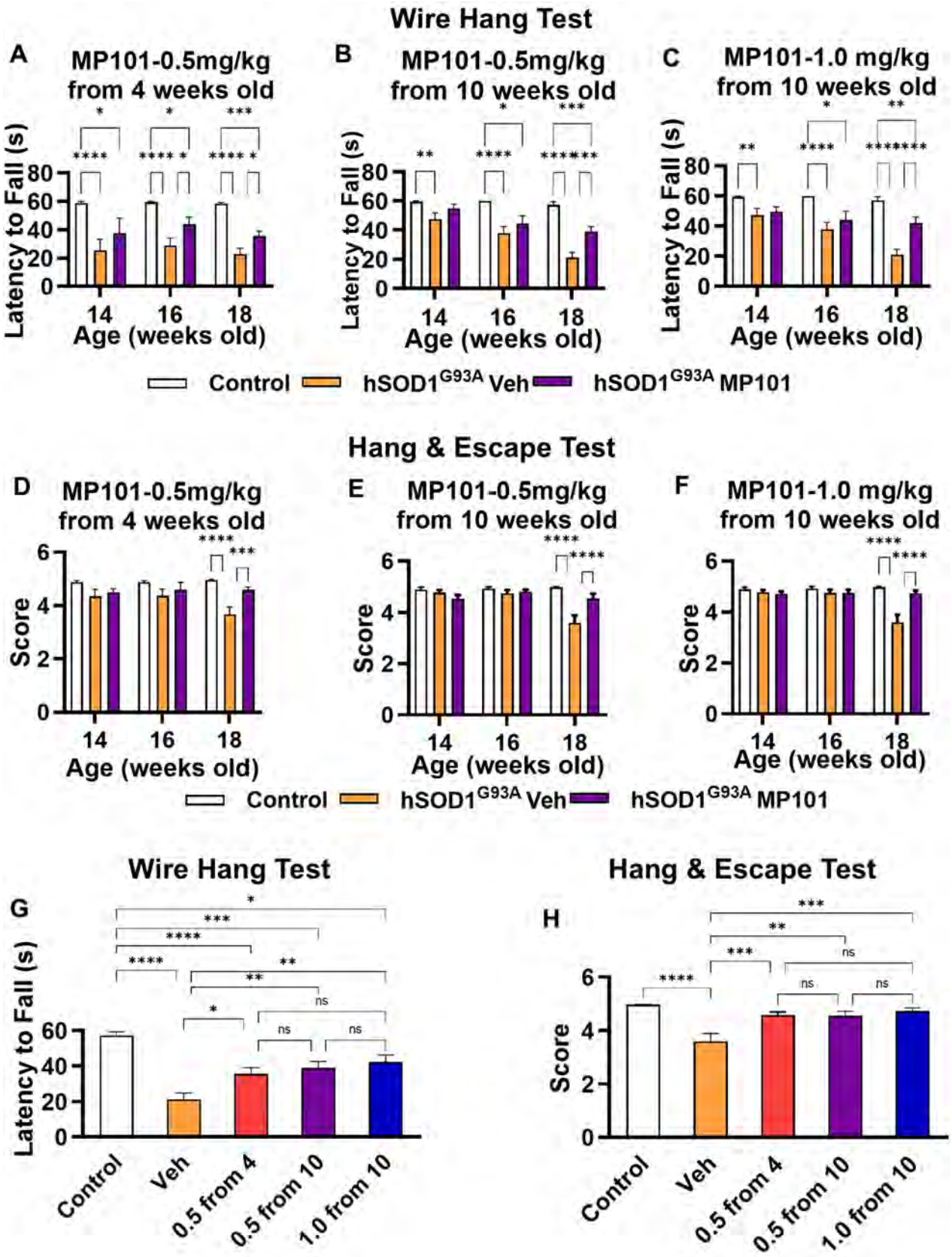

(Figure legend continues on next page.)

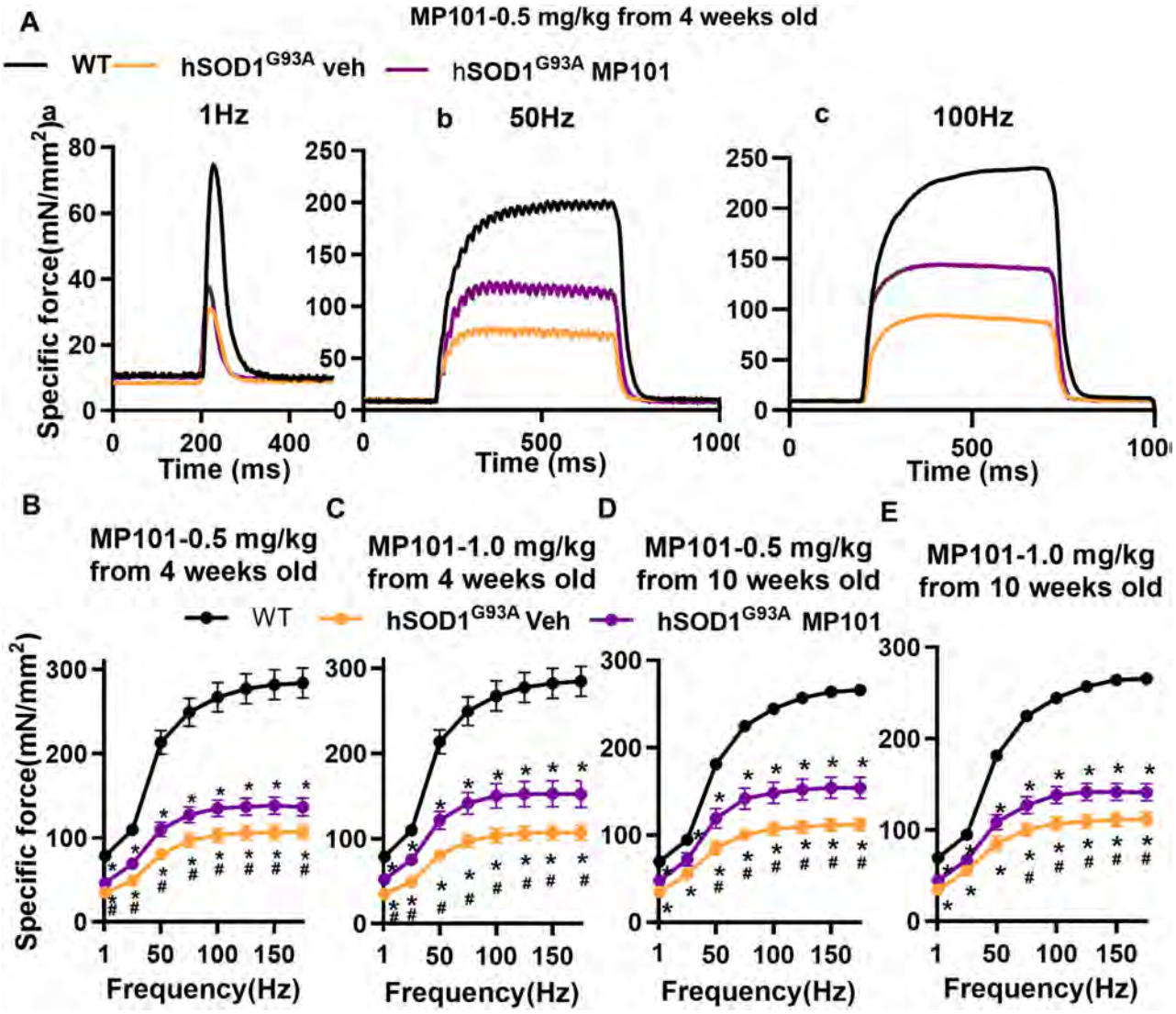

FIGURE 5: MP101 treatment improved muscle contractile force at 18 weeks old in hSOD1^{G93A} mice. (A) Representative traces for in situ muscle contraction in EDL muscles upon twitch stimulation (a), 50 Hz (b), and 100 Hz (c) tetanic stimulation from age/sex matched MP101- and Veh-treated hSOD1^{G93A} and WT mice. (B-E) Force-frequency relationship for EDL muscles subjected to in situ muscle contraction from MP101- and Veh-treated hSOD1^{G93A} mice and control mice started from 4 weeks old (B, 0.5 mg/kg MP101; C, 1.0 mg/kg MP101) and 10 weeks old (D, 0.5 mg/kg MP101; E, 1.0 mg/kg MP101). *$p < 0.05$ versus WT; $^{\#}p < 0.05$ versus MP101, 2-way ANOVA with repeated measures, Tukey post hoc test. N = 7–12 mice (3–4 males and 4–8 females).

sign of MN degeneration in ALS[26] and is clinically related to disease severity and progression.[32] Therefore, MUNE through in situ muscle contraction was conducted in EDL muscles to assess the impact of MP101 administration on MU preservation. EDL muscles from MP101-treated hSOD1^{G93A} mice starting treatment from 4 weeks old showed greater MUNE at 18 weeks old compared with vehicle controls (in Fig 6A, a-c), suggesting a protective role

FIGURE 4: Improved overall muscle strength in hSOD1^{G93A} mice following MP101 treatment from both presymptomatic stage and disease onset. (A) Averaged (±SEM) latency to fall during wire hang tests at 14–18 weeks old in age/sex matched WT and hSOD1^{G93A} mice treated with 0.5 mg/kg MP101 or Veh from 4 weeks old. (B-C) Averaged (±SEM) latency to fall during wire hang tests similar to (A) except for from mice treated with 0.5 mg/kg (B) or 1.0 kg/mg MP101 (C) from 10 weeks old. (D) Averaged (±SEM) scores for hang and escape tasks at 14–18 weeks old in age/sex matched WT and hSOD1^{G93A} mice treated with 0.5 mg/kg MP101 or Veh from 4 weeks old. (E-F) Averaged (±SEM) scores for hang and escape tasks similar to (E) except for from mice treated with 0.5 mg/kg (E) or 1.0 kg/mg MP101 (F) from 10 weeks old. (G) Averaged (±SEM) latency to fall during wire hang tests at 18 weeks old to compare the rescuing effects across different experimental conditions. (H) Averaged (±SEM) scores for hang and escape tasks at 18 weeks old to compare the rescuing effects across different experimental conditions. *$p < 0.05$, **$p < 0.01$, ***$p < 0.001$, 2-way ANOVA with repeated measures, Tukey post hoc test. N = 10–12 mice (4 males and 5–8 females).

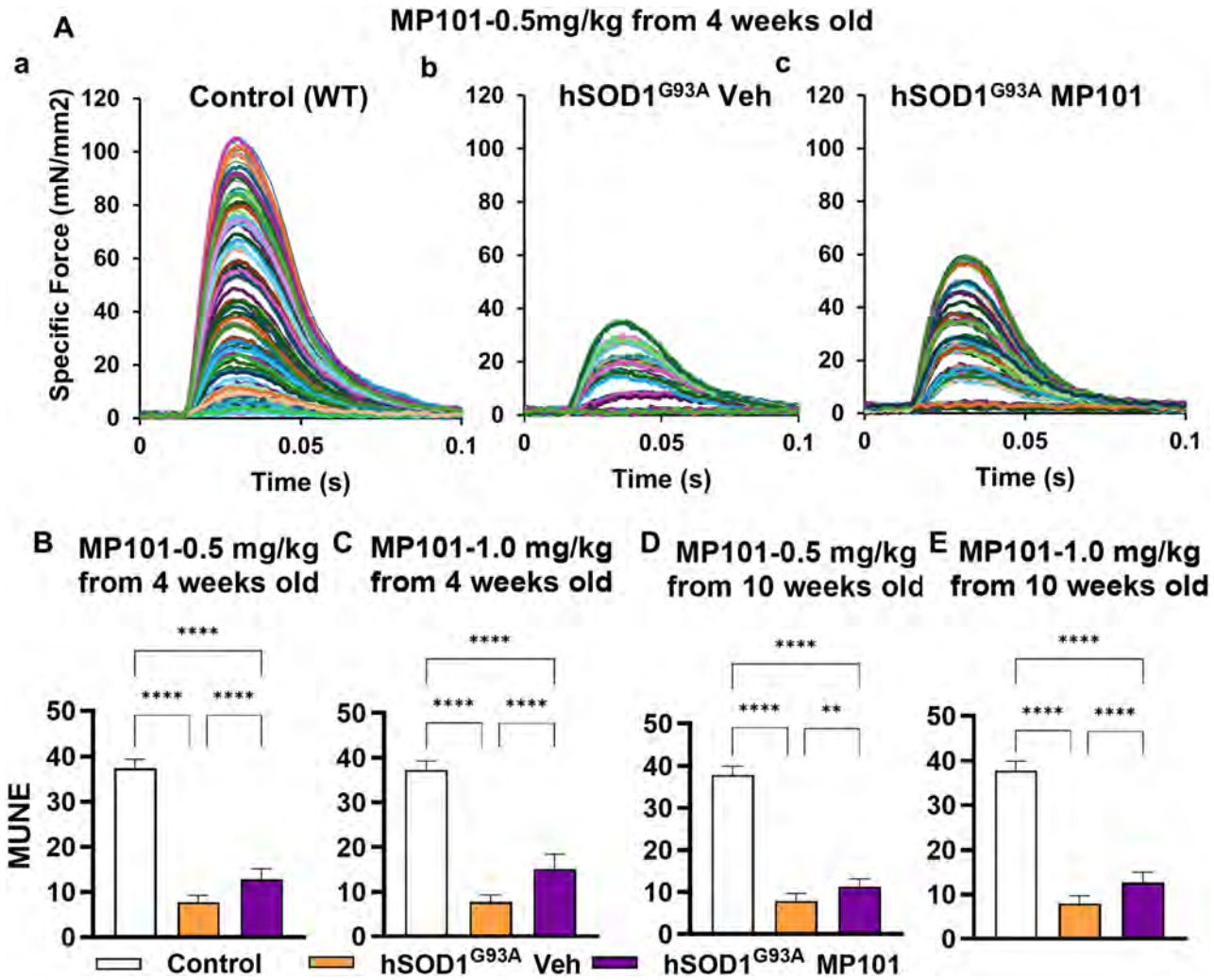

FIGURE 6: MP101 treatment preserved motor unit number at 18 weeks old in hSOD1^{G93A} mice. (A) Representative traces for motor unit number estimation (MUNE) in control (a), Veh- (b), and 0.5 mg/kg MP101- (c) treated WT and hSOD1^{G93A} mice from 4 weeks old. (B-E) Averaged (±SEM) MUNE in EDL muscles from 0.5 mg/kg (B and D) and 1.0 mg/kg (C and E) MP101- and Veh-treated hSOD1^{G93A} mice starting from 4 weeks (B and C) and 10 weeks (D and E) old. *$p < 0.05$, **$p < 0.01$, ***$p < 0.001$, 2-way ANOVA with repeated measures, Tukey post hoc test. N = 10–12 mice (4 males and 5–8 females).

of MP101 treatment from early stage (Fig 6B,C). Treatment of MP101 from disease onset also resulted in an improvement in MUNE at 18 weeks old, at both 0.5 mg/kg and 1.0 mg/kg (Fig 6D,E). Finally, the reduced peak twitch force in EDL from hSOD1^{G93A} mice was also partially restored following MP101 treatment (Fig 6A, a-c).

MP101 Treatment Improved Muscle Innervation and Post-Synaptic NMJ Structure at 18 Weeks Old in hSOD1^{G93A} ALS Mice

The morphology of NMJ pre(neurofilaments) and post-synaptic assembly (AChR) were characterized to determine the protection of MP101 on NMJ structure and muscle innervation. Daily 0.5 mg/kg (Fig 7A, Supplemental Fig 2A) or 1.0 mg/kg (Fig 7B, Supplemental Fig 2B) MP101 treatment in hSOD1^{G93A} mice from 10 weeks old showed significant improvement in muscle innervation and postsynaptic NMJ structure in EDL muscles at 18 weeks old (Fig 7C-F for 0.5 mg/kg; G-J for 1.0 mg/kg), compared with Veh-treated hSOD1^{G93A} mice. Postsynaptic NMJ morphology was less degenerated in treated EDL (Fig 7D and H), with lower percentage of "plaque-like" postsynaptic structure (Fig 7E and I) and decreased fragmentation (≥4 islands in the postsynaptic assembly, Fig 7F and J). Similar results were observed in mice that started treatment with 1.0 mg/ kg MP101 from 4 weeks old (Fig 7K-N).

MP101 Treatment Suppressed Inflammation, Reduced Protein Oxidation, and Promoted Akt Activation in Limb Muscles at 18 Weeks Old in hSOD1^{G93A} ALS Mice

We next explored several possible mechanisms for the protective effects of MP101, using hSOD1^{G93A} mice treated

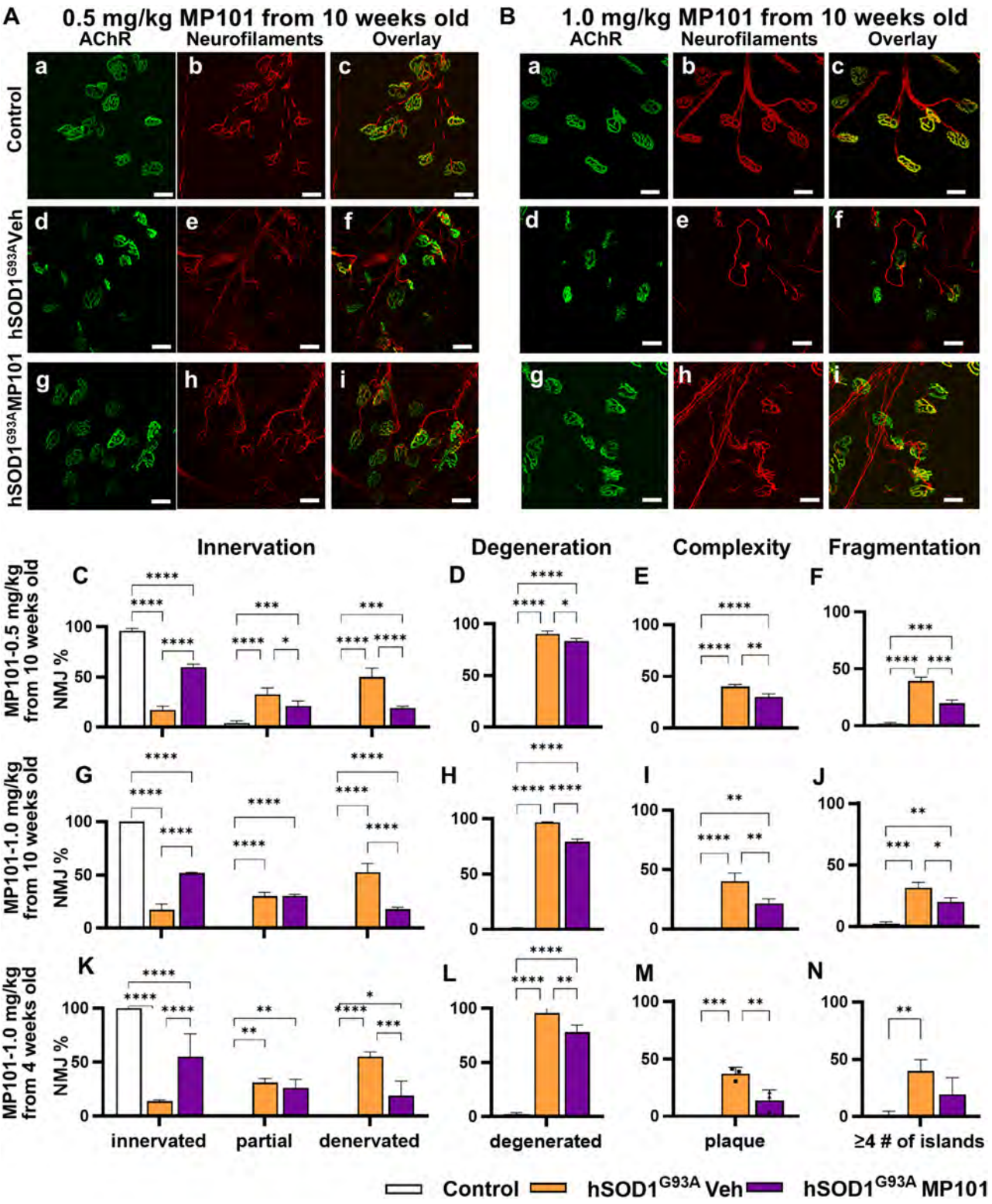

FIGURE 7: MP101 treatment improved EDL muscle innervation and NMJ post-synaptic morphology at 18 weeks old in hSOD1^{G93A} ALS mice. (A-B) Representative images of NMJ stained for post-synaptic AChR (*green*, a, d, g), presynaptic neurofilaments (*red*, b, e, h) and overlay images (c, f, i) in EDL from hSOD1^{G93A} mice treated with 0.5 mg/kg (A) and 1.0 mg/kg (B) MP101 from 10 weeks old. (C-N) Averaged (±SEM) percentage of muscle innervation (C, G, K); postsynaptic degeneration (D, H, L), complexity (E, I, M), and fragmentation (F, J, N) at 18 weeks old in EDL muscles from WT and hSOD1^{G93A} mice following treatment of 0.5 mg/kg MP101 from 10 weeks old (C-F), 1.0 mg/kg MP101 from 10 weeks old (G-J) and 1.0 mg/kg MP101 from 4 weeks old (K-N), respectively. *$p < 0.05$, **$p < 0.01$, ***$p < 0.001$, 2-way ANOVA with repeated measures, Tukey post hoc test. N = 3–5 mice (1–2 males and 2–3 females). Scale bars = 50 μm.

with 0.5 mg/kg MP101 from disease onset, the mice that showed functional recovery. Immunofluorescent staining of CD68 (marker for macrophages) in EDL muscle cryosections revealed a significant increase in the number of CD68+ cells in Veh-treated hSOD1^{G93A} mice at 18 weeks old (Fig 8A a, b and B), which was reversed to WT level following MP101 treatment (Fig 8A-c and B). Further, the level of protein carbonyl (protein oxidation) in Veh-treated hSOD1^{G93A} mice was significantly elevated compared to the control group (Fig 8C,D), while no difference in protein oxidation was detected between MP101-treated hSOD1^{G93A} mice and the control. However, direct comparison between Veh- and MP101-treated hSOD1^{G93A} mice did not reach statistical significance.

Immunoblot analysis showed an overexpression of total Akt protein in the TA muscle of ALS mice, consistent with previous studies.[33] Treatment with MP101 restored total Akt to control level (Fig 8E,F). Interestingly, given the elevated total Akt in hSOD1^{G93A} TA muscle, the activation of Akt, indicated by phosphorylated Akt-Ser473 (p-Akt)/total Akt ratio, was unaltered. MP101 treatment promoted the activation of Akt (Fig 8E and G, increased p-Akt/Akt ratio), potentially supporting muscle growth through the activation of Akt/mTOR (mammalian target of rapamycin) pathway.

Discussion

Mitochondria dysfunction has been reported as one of the early key pathological events in ALS patients and animal models. However, drugs targeting on mitochondrial-related processes have been unsuccessful in modifying the disease phenotype. DNP falls into a unique chemistry class called ionophores/protonophores or uncouplers, and has very wide tissue distribution and brain penetrant as an oral small molecule.[22] The "target" of DNP is the mitochondria itself, not an enzyme or receptor, and modulates the entire organelles physiology. In this study, we thoroughly examined the potential therapeutic effect of DNP (MP101) in improving motor function, muscle contractile function and muscle innervation in hSOD1^{G93A} ALS mouse model. Preserved motor function is highly clinically relevant and will significantly improve the life quality of patients with ALS. The main findings of this study are (1) Both 0.5 mg/kg and 1.0 mg/kg MP101 improved motor coordination and delayed disease progression when starting treatment from both presymptomatic and disease onset; (2) Early treatment of MP101 delayed disease onset; (3) MP101 treatments led to "recovery" of running ability when treatment started at disease onset; (4) MP101 maintained muscle strength both in vivo and in situ; (5) MP101 preserved motor units, improved muscle innervation and postsynaptic NMJ structure in ALS-susceptible EDL muscle; (6) MP101 reduced macrophage infiltration and overall protein oxidation, and enhanced Akt activation in skeletal muscle from ALS mice. Overall, these results provide compelling preclinical evidence supporting the high potential of using MP101 as a novel and promising treatment for ALS.

The most striking finding of this study was that starting MP101 at disease onset promoted a recovery of previous lost skills (running at 20 cm/s). This reversal of motor function following treatment with a small molecule from disease onset has never been reported before. To date, the 3 FDA approved drugs to treat ALS, Riluzole,[5] Edaravone,[6] and AMX0035,[7] show very limited ability in extending lifespan, and no approved drug has shown potential reversal of the disease phenotype. The only treatment that is related to mitochondria, but not directly targeting mitochondrial dysfunction, is AMX0035 (a mixture of sodium phenylbutyrate [PB], and taurursodiol [TURSO]). Both compounds are peri-mitochondria and do not enter the mitochondria. PB is a small molecular chaperone designed to reduce the unfolded protein response or endoplasmic reticulum (ER) stress; and TURSO is a Bcl-2–associated X protein inhibitor, designed to reduce cell death through mitochondrial-related apoptosis.[34,35] Unfortunately, AMX0035 recently did not meet positive outcomes in prolonging survival and improving function in their recent Phase III randomized trial. Other promising candidates for ALS treatment include, but not limited to, Nuedexta, a mixture of dextromethorphan and quinidine (DMQ), a prescription medication treating pseudobulbar affect, showed efficacy to improve bulbar function in patients with ALS in a randomized, blinded, crossover clinical trial using a self-reported grading scale, possibly due to dextromethorphan being an inhibitor of N-methyl-D-aspartate (NMDA) receptor (reducing glutamate excitotoxicity) and a Sigma-1 receptor agonist (stabilizing the interaction and calcium transfer between ER and mitochondria and reducing ER stress).[36] Therefore, a thorough evaluation of Nuedexta's efficacy on motor function is warranted. Another Sigma-1 receptor agonist, SA4503, and GNX-4728, an inhibitor of mPTP both improved ALS phenotype in preclinical studies, but yet to be tested in the human population.[37,38] No functional recoveries were reported in these preclinical studies. Overall, the marked improvement in motor and muscle function with potential recovery of the disease phenotype in MP101-treated ALS mice in this study lend strong support of using MP101 as a new drug for ALS, by modulating the entire mitochondrial organelle's physiology to pro-survival.

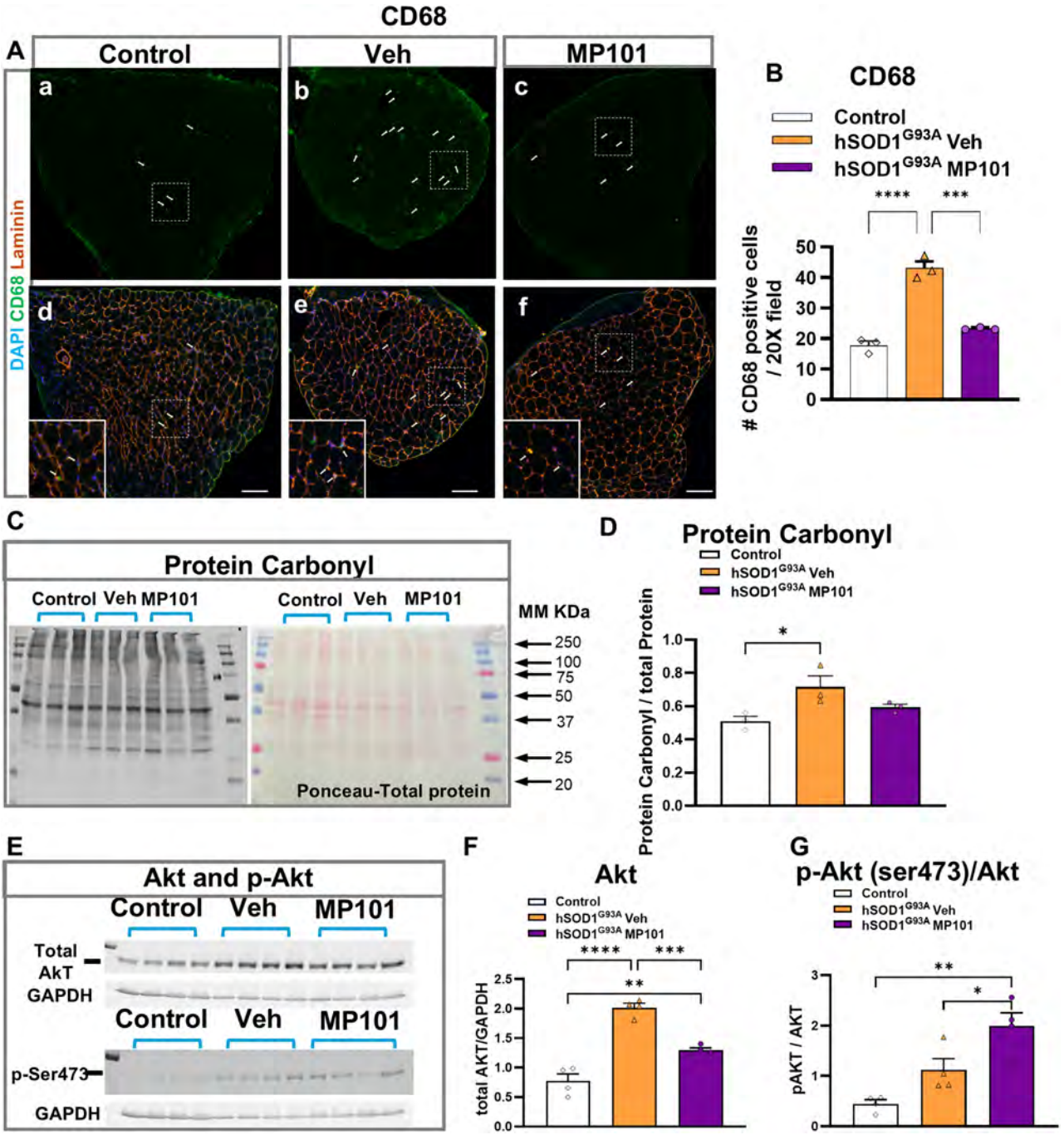

FIGURE 8: 0.5 mg/kg MP101 treatment from 10 weeks old suppressed inflammation, reduced protein oxidation, and increased the phosphorylation of Akt in skeletal muscles at 18 weeks old in hSOD1^{G93A} ALS mice. (A) Representative immunofluorescent images of CD68 staining (*green*) in EDL muscle sections from control (a, d), veh- (b, e), and MP101-treated (c, f) mice., co-labeled with laminin (*orange*) and DAPI (nuclei, *blue*) to show localization. White arrows indicate example CD68 positive cells. Scale bars = 150 μm. Insets: high magnification images of boxed regions. (B) Averaged (±SEM) number of CD68 positive cells per 20× field. (C) Immunoblot (Oxyblot) images following Protein Carbonyl assay in TA muscle lysate, with ponceau total protein stain (right) as loading control. (D) Averaged (±SEM) intensity of protein oxidation using densitometry analysis. (E) Immunoblot images for total Akt and phosphorylated Akt (p-AkT Ser473), with GAPDH as loading control. (F-G) Averaged (±SEM) densitometry analysis on protein levels of total Akt (F) and pAkt/Akt ratios (G). *$p < 0.05$, **$p < 0.01$, ***$p < 0.001$, ****$p < 0.0001$, 2-way ANOVA with repeated measures, Tukey post hoc test. N = 3–4 mice (1–2 males and 2 females).

In addition to Ca^{2+} induced mitochondrial dysfunction, oxidative stress has been the dogma for ALS pathogenesis for decades. Presynaptic components of the NMJ are particularly sensitive to ROS-induced damage, supporting the idea that ROS is a mechanism that contributes to NMJ destruction.[39] Antioxidant reactive

element (ARE), a cis-regulatory enhancer sequence found in the promoter region of several genes involved in the detoxification mechanism and activated by oxidative stress,[40] is activated to a greater extent in gastrocnemius muscles in hSOD1^{G93A} mice at 30 days old,[41] indicating an early contribution of oxidative stress in the ALS phonotype. Mitochondrial ROS production is the main source of cellular ROS and exhibits a sharp positive correlation with $\Delta\Psi_m$.[42] Proton leak (mild uncoupling of $\Delta\Psi_m$) is viewed as a protective process to limit ROS-induced damage in all cell types.[43] Indeed, results in this study showed reduced overall protein oxidation, suggesting reduced oxidative stress in MP101-treated muscles. Therefore, slightly dissipating $\Delta\Psi_m$ may serve as an effective therapeutic approach for neurodegenerative conditions. Daily use of low doses of MP101 (0.5-5 mg/kg in mice) prevented neuronal loss, improved motor coordination, and reduced oxidative stress in mouse models of several neurodegenerative conditions.[23,44–46] Therefore, Mitochon Pharmaceuticals, Inc. repositioned MP101 as a disease-modifying drug and was granted an open Investigational New Drug (IND) approval by the FDA.[22] In addition, the European Medicines Agency has approved an sALS biomarker study currently underway in Europe with MP101.

The mechanism-of-action (MOA) for the protective effect of MP101 in ALS mice, as we observed in this study, and in other neurodegenerative conditions requires further investigation. Several possible aspects of MP101's pleiotropic pharmacology are likely to provide a benefit. First, a reduction in $\Delta\Psi_m$ in damaged mitochondria may facilitate the turnover of the mitochondria to be replaced by healthy mitochondria (mitochondrial renewal). Second, slightly dissipating $\Delta\Psi_m$ of relatively healthy mitochondria reduces Ca^{2+}-induced mitochondrial dysfunction and ROS generation, and therefore provides protection. Third, apart from the traditional role of MP101 as a protonophore/ionophore, micro-dose MP101 alters the activation of Akt/mTOR pathway.[21] Our finding of reduced total Akt expression and enhanced Akt activation indicate the potential involvement of Akt/mTOR pathway in the functional improvement of MP101-treated ALS mice, given that Akt/mTOR pathway is the primary pathway mediating muscle growth. These results are also in accordance with a recent study that showed decreased p-Akt/Akt ratio in ALS mice, while swimming training decreased total Akt, increased pAkt/Akt ratio in skeletal muscles and improved muscle function.[47] Fourth, the functional improvement in MP101-treated hSOD1^{G93A} mice may be attributed to attenuated inflammation seen in the current and prior multiple sclerosis study,[44] indicated by reduced macrophage infiltration. Finally, MP101 stimulates the cAMP-response element-binding protein-BDNF cascade, which is essential for synaptic plasticity, adaptive stress responses and cognitive function.[48] Collectively, these features of the pharmacology of MP101 all likely play a role. However, titrating which ones are the most beneficial requires much deeper exploration. Mitochondria population exists within the cell in a symbiotic relationship providing energy for the cell and core to cellular health, so it may not seem surprising that targeting the mitochondria directly and specifically with MP101 to lower damage and promote repair benefits a legion of diseases rooted in mitochondrial dysfunction.[22]

Destruction of NMJ represents an early event in ALS disease progression ("distal axonopathy"). Therefore, muscle innervation and skeletal muscle function are essential readout of the effect of therapeutic drugs for ALS. While global structural and functional improvements in NMJ and skeletal muscle were observed in hSOD1^{G93A} mice treated with 0.5 mg/kg MP101, no further improvement was detected when increasing the dose to 1.0 mg/kg. This result indicates that MP101 exerts its effect with high efficacy and only "micro-dose" is needed to obtain its beneficial effect in ALS mice. Certainly, this dosage is most likely disease specific. Previous study showed maximal rescue of disease phenotype in a multiple sclerosis animal model using 5 mg/kg MP101,[44] instead of the lower doses used in the current study, indicating that the mitochondria in ALS mice might be more sensitive to membrane depolarization. Therefore, it might be informative to examine lower doses such as 0.25 mg/kg in ALS models in future studies. Regardless of the dosages, the significant rescue in ALS disease phenotype when MP101 treatment was started after disease onset provides critical proof-of-concept evidence of using mitochondria as a therapeutic target and MP101 as a therapeutic drug for ALS. Due to the significant heterogeneity of disease biology between humans with ALS and ALS animal models, we remain conservative on the possible impact of MP101 in a clinical setting. However, the high conservation of mitochondrial physiology among mammals does provide MP101 with some advantage moving from mouse to human. Further, ALS is a multisystem, non-autonomic condition, and additional drugs that complement the benefits seen here are prudent, such that a multitarget cocktail may provide optimal outcomes for the treatment of this condition. In this study, we used hSOD1^{G93A} mice on a C57Bl6 background, which does not exhibit sexual dimorphism. Considering that sex is one of the risk factors for patients with ALS[49] and previous studies reported sex-dependent differential responses to treatment in ALS animal models,[50] this can be a limitation of this study. Future study is also needed to assess the efficacy of MP101 in a

sporadic model, such as TDP-43 mouse models. Nonetheless, if the functional reversal of MP101 in ALS mice can be successfully translated to a clinical setting, whether by itself or in combination with other interventions, this can possibly be a life-changing treatment for patients with ALS and other MN degenerative conditions.

Acknowledgments

This study was supported by research grant NIH/NINDS NS99545, NS117429, and NS127858 to L.W.-L.

Author Contributions

R.Z. and L.W.-L. contributed to the conception and design of the study; R.Z., D.L.A.D., N.K., E.N.R., and L.W.-L. contributed to the acquisition and analysis of data; R.Z., J.G.G., and L.W.-L. contributed to drafting the text or preparing the figures.

Potential Conflicts of Interest

J.G.G. is the Chief Scientific Officer, a Co-founder and shareholder of Mitochon Pharmaceuticals Inc., a for-profit company and the manufacturer of MP101 used in this study.

Data Availability

The data that support the findings of this study are available from the corresponding author upon reasonable request.

References

1. Kwiatkowski TJ, Bosco DA, Leclerc AL, et al. Mutations in the FUS/TLS gene on chromosome 16 cause familial amyotrophic lateral sclerosis. Science 2009;323:1205–1208.
2. Kabashi E, Valdmanis PN, Dion P, et al. TARDBP mutations in individuals with sporadic and familial amyotrophic lateral sclerosis. Nat Genet 2008;40:572–574.
3. Renton AE, Majounie E, Waite A, et al. A hexanucleotide repeat expansion in C9ORF72 is the cause of chromosome 9p21-linked ALS-FTD. Neuron 2011;72:257–268.
4. Rosen DR, Siddique T, Patterson D, et al. Mutations in Cu/Zn superoxide dismutase gene are associated with familial amyotrophic lateral sclerosis. Nature 1993;362:59–62.
5. Bensimon G, Lacomblez L, Meininger V. A controlled trial of riluzole in amyotrophic lateral sclerosis. N Engl J Med 1994;330:585–591.
6. Abe K, Aoki M, Tsuji S, et al. Safety and efficacy of edaravone in well defined patients with amyotrophic lateral sclerosis: a randomised, double-blind, placebo-controlled trial. Lancet Neurol 2017;16:505–512.
7. Paganoni S, Hendrix S, Dickson SP, et al. Long-term survival of participants in the CENTAUR trial of sodium phenylbutyrate-taurursodiol in amyotrophic lateral sclerosis. Muscle Nerve 2021;63:31–39.
8. Miller TM, Cudkowicz ME, Genge A, et al. Trial of antisense oligonucleotide tofersen for *SOD1* ALS. N Engl J Med 2022;387:1099–1110.
9. Chung MJ, Suh YL. Ultrastructural changes of mitochondria in the skeletal muscle of patients with amyotrophic lateral sclerosis. Ultrastruct Pathol 2002;26:3–7.
10. Crugnola V, Lamperti C, Lucchini V, et al. Mitochondrial respiratory chain dysfunction in muscle from patients with amyotrophic lateral sclerosis. Arch Neurol 2010;67:849–854.
11. Russell AP, Wada S, Vergani L, et al. Disruption of skeletal muscle mitochondrial network genes and miRNAs in amyotrophic lateral sclerosis. Neurobiol Dis 2013;49:107–117.
12. Damiano M, Starkov AA, Petri S, et al. Neural mitochondrial Ca^{2+} capacity impairment precedes the onset of motor symptoms in G93A Cu/Zn-superoxide dismutase mutant mice. J Neurochem 2006;96:1349–1361.
13. Luo G, Yi J, Ma C, et al. Defective mitochondrial dynamics is an early event in skeletal muscle of an amyotrophic lateral sclerosis mouse model. PLoS One 2013;8:e82112.
14. Zhou J, Yi J, Fu R, et al. Hyperactive intracellular calcium signaling associated with localized mitochondrial defects in skeletal muscle of an animal model of amyotrophic lateral sclerosis. J Biol Chem 2010;285:705–712.
15. Marchioretti C, Zanetti G, Pirazzini M, et al. Defective excitation-contraction coupling and mitochondrial respiration precede mitochondrial Ca. Nat Commun 2023;14:602.
16. Abeti R, Abramov AY. Mitochondrial Ca^{2+} in neurodegenerative disorders. Pharmacol Res 2015;99:377–381.
17. Geisler JG, Marosi K, Halpern J, Mattson MP. DNP, mitochondrial uncoupling, and neuroprotection: a little dab'll do ya. Alzheimers Dement 2017;13:582–591.
18. De Felice FG, Ferreira ST. Novel neuroprotective, neuritogenic and anti-amyloidogenic properties of 2,4-dinitrophenol: the gentle face of Janus. IUBMB Life 2006;58:185–191.
19. Lee Y, Heo G, Lee KM, et al. Neuroprotective effects of 2,4-dinitrophenol in an acute model of Parkinson's disease. Brain Res 2017;1663:184–193.
20. Pandya JD, Pauly JR, Nukala VN, et al. Post-injury administration of mitochondrial uncouplers increases tissue sparing and improves behavioral outcome following traumatic brain injury in rodents. J Neurotrauma 2007;24:798–811.
21. Liu D, Zhang Y, Gharavi R, et al. The mitochondrial uncoupler DNP triggers brain cell mTOR signaling network reprogramming and CREB pathway up-regulation. J Neurochem 2015;134:677–692.
22. Geisler JG. 2,4 dinitrophenol as medicine. Cells 2019;8:280.
23. Wu B, Jiang M, Peng Q, et al. 2,4 DNP improves motor function, preserves medium spiny neuronal identity, and reduces oxidative stress in a mouse model of Huntington's disease. Exp Neurol 2017;293:83–90.
24. Matsuo N, Tanda K, Nakanishi K, et al. Comprehensive behavioral phenotyping of ryanodine receptor type 3 (RyR3) knockout mice: decreased social contact duration in two social interaction tests. Front Behav Neurosci 2009;3:3.
25. Loy RE, Orynbayev M, Xu L, et al. Muscle weakness in Ryr1I4895T/WT knock-in mice as a result of reduced ryanodine receptor Ca2+ ion permeation and release from the sarcoplasmic reticulum. J Gen Physiol 2011;137:43–57.
26. Acevedo-Arozena A, Kalmar B, Essa S, et al. A comprehensive assessment of the SOD1G93A low-copy transgenic mouse, which models human amyotrophic lateral sclerosis. Dis Model Mech 2011;4:686–700.
27. Falk DJ, Todd AG, Lee S, et al. Peripheral nerve and neuromuscular junction pathology in Pompe disease. Hum Mol Genet 2015;24:625–636.
28. Valdez G, Tapia JC, Kang H, et al. Attenuation of age-related changes in mouse neuromuscular synapses by caloric restriction and exercise. Proc Natl Acad Sci U S A 2010;107:14863–14868.

29. Ainbinder A, Boncompagni S, Protasi F, Dirksen RT. Role of Mitofusin-2 in mitochondrial localization and calcium uptake in skeletal muscle. Cell Calcium 2015;57:14–24.

30. Laitano O, Pindado J, Valera I, et al. The impact of hindlimb disuse on sepsis-induced myopathy in mice. Physiol Rep 2021;9:e14979.

31. Chou C-H, Barton ER. Phosphorylation of AMPKα at Ser485/491 is dependent on muscle contraction and not muscle-specific IGF-I overexpression. Int J Mol Sci 2023;24:11950.

32. Ahn SW, Kim SH, Oh DH, et al. Motor unit number estimation in evaluating disease progression in patients with amyotrophic lateral sclerosis. J Korean Med Sci 2010;25:1359–1363.

33. Querfurth H, Lee HK. Mammalian/mechanistic target of rapamycin (mTOR) complexes in neurodegeneration. Mol Neurodegener 2021; 16:44.

34. Kusaczuk M. Tauroursodeoxycholate-bile acid with chaperoning activity: molecular and cellular effects and therapeutic perspectives. Cells 2019;8:1471.

35. Ryu H, Smith K, Camelo SI, et al. Sodium phenylbutyrate prolongs survival and regulates expression of anti-apoptotic genes in transgenic amyotrophic lateral sclerosis mice. J Neurochem 2005;93: 1087–1098.

36. Smith R, Pioro E, Myers K, et al. Enhanced bulbar function in amyotrophic lateral sclerosis: the Nuedexta treatment trial. Neurotherapeutics 2017;14:762–772.

37. Rodríguez LR, Lapeña-Luzón T, Benetó N, et al. Therapeutic strategies targeting mitochondrial calcium signaling: a new hope for neurological diseases? Antioxidants (Basel) 2022;11:165.

38. Ono Y, Tanaka H, Takata M, et al. SA4503, a sigma-1 receptor agonist, suppresses motor neuron damage in in vitro and in vivo amyotrophic lateral sclerosis models. Neurosci Lett 2014;559: 174–178.

39. Naumenko N, Pollari E, Kurronen A, et al. Gender-specific mechanism of synaptic impairment and its prevention by GCSF in a mouse model of ALS. Front Cell Neurosci 2011;5:26.

40. Rushmore TH, Morton MR, Pickett CB. The antioxidant responsive element. Activation by oxidative stress and identification of the DNA consensus sequence required for functional activity. J Biol Chem 1991;266:11632–11639.

41. Kraft AD, Resch JM, Johnson DA, Johnson JA. Activation of the Nrf2-ARE pathway in muscle and spinal cord during ALS-like pathology in mice expressing mutant SOD1. Exp Neurol 2007;207: 107–117.

42. Korshunov SS, Skulachev VP, Starkov AA. High protonic potential actuates a mechanism of production of reactive oxygen species in mitochondria. FEBS Lett 1997;416:15–18.

43. Brand MD. Uncoupling to survive? The role of mitochondrial inefficiency in ageing. Exp Gerontol 2000;35:811–820.

44. Bando Y, Geisler JG. Disease modifying mitochondrial uncouplers, MP101, and a slow release ProDrug, MP201, in models of multiple sclerosis. Neurochem Int 2019;131:104561.

45. Khan RS, Dine K, Geisler JG, Shindler KS. Mitochondrial uncoupler prodrug of 2,4-dinitrophenol, MP201, prevents neuronal damage and preserves vision in experimental optic neuritis. Oxid Med Cell Longev 2017;2017:10.

46. Kishimoto Y, Johnson J, Fang W, et al. A mitochondrial uncoupler prodrug protects dopaminergic neurons and improves functional outcome in a mouse model of Parkinson's disease. Neurobiol Aging 2020;85:123–130.

47. Halon-Golabek M, Flis DJ, Zischka H, et al. Amyotrophic lateral sclerosis associated disturbance of iron metabolism is blunted by swim training-role of AKT signaling pathway. Biochim Biophys Acta Mol Basis Dis 2024;1870:167014.

48. Kandel ER, Dudai Y, Mayford MR. The molecular and systems biology of memory. Cell 2014;157:163–186.

49. Zamani A, Thomas E, Wright DK. Sex biology in amyotrophic lateral sclerosis. Ageing Res Rev 2024;95:102228.

50. Bankole O, Scambi I, Parrella E, et al. Beneficial and sexually dimorphic response to combined HDAC inhibitor valproate and AMPK/SIRT1 pathway activator resveratrol in the treatment of ALS mice. Int J Mol Sci 2022;23:1047.